Asymmetric Compressive Stability of Rotating Annular Plates

H. Bagheri[1], Y. Kiani[2,*] and M. R. Eslami[1]

[1]*Mechanical Engineering Department, Amirkabir University of Technology, Tehran, Iran*
[2]*Faculty of Engineering, Shahrekord University, Shahrekord, Iran*
E-mail: y.kiani@aut.ac.ir
[*]*Corresponding Author*

Received 11 June 2018; Accepted 18 December 2018;
Publication 16 January 2019

Abstract

In the present research, buckling behaviour of an isotropic homogeneous rotating annular plate subjected to uniform compression on both inner and outer edges is analysed. It is further assumed that the plate is rotating with a constant angular speed. Formulation is based on the first order shear deformation plate theory, which is valid for thin and moderately thick plates. The complete set of equilibrium equations and the associated boundary conditions are obtained for the plate. Prebuckling loads of the plate are obtained under flatness and axisymmetric deformations. Using the adjacent equilibrium criterion, the linearised stability equations are extracted. An asymmetric stability analysis is performed to obtain the critical buckling loads of the plate and the buckled configurations of the rotating plate. To this end, trigonometric functions through the circumferential direction and the generalised differential quadrature discretization across the radial direction are used which result in an algebraic eigenvalue problem. Benchmark results are given in graphical presentations for combinations of free, simply-supported, sliding supported, and clamped types of boundary conditions. It is shown that rotation enhances the buckling loads of the plate for all types of boundary conditions and alters the buckled shape of the plate.

European Journal of Computational Mechanics, Vol. 28_4, 325–350.
doi: 10.13052/ejcm1958-5829.2843

Keywords: Annular plate, rotation, uniform compression, generalised differential quadrature.

1 Introduction

Plates with annular shape have different applications in mechanical and civil engineering. The fact that stress distribution in rotating discs may cause fractures and may therefore lead to failures of spinning mechanical systems has become of quite some interest. The regime of stresses induced by rotating may be compressive or tensile depending on the boundaries of the disk. Rotating disks and plates have shown different applications such as, pump rotors, compressors and computer disks. Yamaki (1985) was the first who considered the asymmetrical buckling of annular plates under uniform compression on both edges of the plate. In the analysis of Yamaki (1985) asymmetrical deformations of the plate under axisymmetric loading are taken into consideration. It is found that the buckling loads are often appearing in shapes with one or more nodal diameters. He obtained the buckling loads for twelve combinations of boundary conditions and discussed the stability criteria for the case of small cores. Majumdar (1971) discussed theoretically and experimentally, the buckling of a circular annular plate where the outer edge is clamped and the inner edge is free. The plate is loaded with uniform radial compressive force applied at the outside edge. The solutions indicate that for small ratios of inner to outer radius, the plate buckles into a radially symmetric mode. When the ratio of the inner to outer radius exceeds a certain value, the minimum buckling load corresponds to buckling modes with waves along the circumference. The number of waves depends on the ratio of the inner and the outer radii. Irie et al. (1982) studied the free vibration and stability of a variable thickness annular plate subjected to a torque by the Ritz method. For this purpose, the transverse deflection of an annular plate of a uniform thickness without the action of a torque is written in form of a series of deflection functions. The kinetic and strain energies of the plate are evaluated analytically and the frequency equation of the plate is derived by the conditions for a stationary value of the Lagrange functional. The present method is applied to annular plates with two types of radial thickness variation, power law and exponential. The natural frequencies and the divergence torques are calculated numerically, from which the effects of the varying thickness, inner/outer radii ratio, and edge conditions are studied. Kiani and Eslami (2013a) obtained the critical buckling temperatures of annular plates made

from a functionally graded material. The plate is assumed to be attached to an elastic medium which acts as an elastic foundation. Formulation is limited to thin plates and asymmetrical stability analysis is performed. It is shown that the fundamental buckling pattern of plates with both edges clamped is always asymmetric. Ghiasian et al. (2014) carried out an investigation on critical buckling temperatures of functionally graded material plates. This study is developed based on a first order shear deformation plate theory which is suitable for thin and moderately thick plates.

Mostaghel and Tadjbakhsh (1973) obtained a closed-form formula for critical speed of a spinning solid circular plate where the edge of the plate is restrained against radial expansion. In this analysis, rotating angular speed is assumed to be constant and solution method is based on the Coulomb wave functions. Iwan and Moeller (1976) discussed the effect of a transverse load on the stability of a spinning elastic disk. The disk rotates with a constant angular velocity and the load consists of a mass distributed over a small area of the disk with a spring and a dashpot. The equation of motion for the transverse vibration of the disk is written as a system of linear ordinary differential equations with constant coeffcients. The analysis indicates that the disk system is unstable for speeds in a region above the critical speeds of vibration of the spinning disk due to the effects of load stiffness. The mass and damping of the load system cause a terminal instability and other instabilities occur as a result of modal interaction.

Eid and Adams (2006) obtained the critical speeds of a moderately thick circular spinning disk by using the Mindlin plate theory, which includes shear deformation and rotational inertia. A combination of analytical and numerical methods is used to calculate the four lowest critical speeds for a centrally clamped uniform circular disk. Comparisons between the critical speeds of the shear deformable plate with those of classical plate theory, which neglects shear deformation and rotational inertia, are made. Maretic (1998) analyzed the vibration and stability of a circular plate with elastically restrained edge induced due to the rotation with constant angular velocity. Maretic et al. (2007) analyzed the vibration and stability of a circular plate induced due to the rotation with constant angular velocity and a constant external torque. The buckled states of an annular plate under the simultaneous action of an edge torque and constant angular velocity are obtained. In this analysis asymmetric formulation is presented. Stability analysis is performed using the adjacent equilibrium criterion. Annular plates with both edges clamped are considered and solution method is based on the Galerkin method. Solution method of this

research, however, is restricted to thin plates. Maretic and Glavardanov (2004) discussed the linear and nonlinear stability of a solid thin rotating circular plate subjected to uniform temperature rise loading. Stress redistribution and critical states of rotating solid circular plates are analyzed by Tutunku (2000) and Tutunku and Durdu (1998). In the mentioned works, finite element formulation is applied to obtain the critical speed of the plate. As concluded in these researches, increasing the orientation up to a certain point makes the plate less stable. Adams (1987) modelled the rotation of floppy disk with a spinning annular plate and extracted the critical states of floppy disk. In this analysis, the elastic foundation model is proposed to postpone the critical state of a rotating floppy disk. As shown in this research, certain critical speeds exist at which the spinning disk is unable to support arbitrary spatially fixed transverse loads. These critical speeds are in the range of rotational speeds relevant to certain floppy disk in magnetic recording applications. The effects of various boundary conditions on the buckling velocity is discussed by Bauer and Eidel (2007). Kiani and Eslami (2014) discussed the nonlinear stability of a functionally graded material solid circular plate subjected to uniform temperature rise and constant rotational speed. This research is limited to axisymmetric deformations. Due to the stretching-bending coupling effects in functionally graded material plates, various nonlinear responses are observed among the results. Recently, Bagheri et al. (2017a) analysed the effects of uniform rotation on the critical buckling temperature of the annular plates and showed that critical buckling temperature of the plate may be enhances under certain circumstances.

To the best of the present authors knowledge and as the above literature survey reveals, the bifurcation buckling of an annular plate subjected to the combined action of rotation and compression is not reported so far. In the present research, first order shear deformation plate theory is used to obtain the critical buckling loads of an annular plate rotating with constant angular speed. To this end, pre-buckling forces of the plate are obtained by using the flatness and axisymmetric deformation conditions. Afterwards, adjacent equilibrium criterion is used to obtain the stability equations. Asymmetrical stability analysis is performed and the governing equations are discreted by means of the generalised differential quadratures. Various types of boundary conditions as combinations of clamped, free, simply supported, and sliding supported are considered. Numerical results are provided in graphical presentation to obtain the critical buckling loads of annular plates as functions of boundary conditions, inner to outer radius ratio, thickness to outer radius ratio and

rotating speed. It is shown that rotation enhances the buckling loads of an annular plate in all cases. However, it may change the buckling pattern of the plate.

2 Theoretical Formulation

Consider an annular plate of thickness h, inner radius b, and outer radius a as shown in Figure 1. The plate is subjected to uniform compression on both inner and outer edges and also rotates with a constant angular speed ω. Polar coordinates system (r, θ, z) with its origin located at the centre of the plate mid-surface is defined. In this system, r, θ, and z represent, respectively, the radial, circumferential, and through-the-thickness directions.

2.1 Kinematic Assumptions

Displacement field in the plate domain is assumed to obey the first order shear deformation plate theory (FSDT). Based on the FSDT, the displacement components of the plate may be written as (Ghiasian et al., 2014)

$$\begin{aligned} u(r,\theta,z) &= u_0(r,\theta) + z\phi_r(r,\theta) \\ v(r,\theta,z) &= v_0(r,\theta) + z\phi_\theta(r,\theta) \\ w(r,\theta,z) &= w_0(r,\theta) \end{aligned} \tag{1}$$

where in Equation (1) u_0, v_0, and w_0 represent the displacements at the mid-surface of the annular plate in the r-, θ-, and z-directions, respectively. Also, ϕ_r and ϕ_θ denote, respectively, the transverse normal rotations about θ and

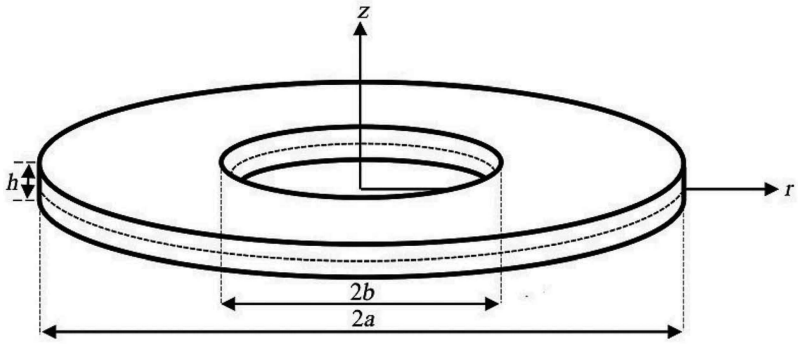

Figure 1 Coordinate system and geometry of an annular plate.

r axes. Besides, a comma indicates the partial derivative with respect to its afterwards.

2.2 Nonlinear Strain-displacement Equations

The von Kármán type of geometrical nonlinearity, consistent with the small strains, moderate rotations, and large displacements in the polar coordinates system takes the form (Ghiasian et al., 2014)

$$\begin{aligned}
\varepsilon_{rr} &= u_{,r} + \frac{1}{2}w_{,r}^2 \\
\varepsilon_{\theta\theta} &= \frac{1}{r}u + \frac{1}{r}v_{,\theta} + \frac{1}{2r^2}w_{,\theta}^2 \\
\gamma_{r\theta} &= \frac{1}{r}u_{,\theta} + v_{,r} - \frac{1}{r}v + \frac{1}{r}w_{,\theta}w_{,r} \\
\gamma_{rz} &= u_{,z} + w_{,r} \\
\gamma_{z\theta} &= \frac{1}{r}w_{,\theta} + v_{,z}
\end{aligned} \tag{2}$$

where ε_{rr} and $\varepsilon_{\theta\theta}$ express the radial and circumferential normal strains and $\gamma_{r\theta}, \gamma_{rz}$, and $\gamma_{z\theta}$ denote the shear strain components.

2.3 Constitutive Equations

When the material of the plate is linearly elastic, the constitutive law for a plane-stress plate exposed to compressive and rotational loadings is (Ghiasian et al., 2014)

$$\begin{Bmatrix} \sigma_{rr} \\ \sigma_{\theta\theta} \\ \tau_{r\theta} \\ \tau_{rz} \\ \tau_{z\theta} \end{Bmatrix} = \begin{bmatrix} Q_{11} & Q_{12} & 0 & 0 & 0 \\ Q_{12} & Q_{22} & 0 & 0 & 0 \\ 0 & 0 & Q_{44} & 0 & 0 \\ 0 & 0 & 0 & Q_{55} & 0 \\ 0 & 0 & 0 & 0 & Q_{66} \end{bmatrix} \begin{Bmatrix} \varepsilon_{rr} \\ \varepsilon_{\theta\theta} \\ \gamma_{r\theta} \\ \gamma_{rz} \\ \gamma_{z\theta} \end{Bmatrix} \tag{3}$$

where $Q_{ij}, i, j = 1, 2, 4, 5, 6$ are the material stiffness coefficients. For an isotropic homogeneous medium under plane stress conditions, these constants are obtained as

$$Q_{11} = Q_{22} = \frac{E}{1 - v^2},\ Q_{12} = vQ_{11},\ Q_{44} = Q_{55} = Q_{66} = \frac{E}{2(1 + v)} \tag{4}$$

2.4 Stress Resultants

Based on the FSDT, the stress resultants are related to the stress components through the following equations (Reddy, 2003)

$$\begin{aligned}(N_{rr}, N_{\theta\theta}, N_{r\theta}) &= \int_{-h/2}^{+h/2} (\sigma_{rr}, \sigma_{\theta\theta}, \tau_{r\theta}) dz \\ (M_{rr}, M_{\theta\theta}, M_{r\theta}) &= \int_{-h/2}^{+h/2} z(\sigma_{rr}, \sigma_{\theta\theta}, \tau_{r\theta}) dz \\ (Q_r, Q_\theta) &= \int_{-h/2}^{+h/2} (\tau_{rz}, \tau_{z\theta}) dz\end{aligned} \tag{5}$$

Substituting Equation (3) into Equation (5) with the aid of Equations (1) and (2), generate the stress resultants in terms of the mid-plane displacements as

$$\begin{Bmatrix} N_{rr} \\ N_{\theta\theta} \\ N_{r\theta} \end{Bmatrix} = \begin{bmatrix} A_{11} & A_{12} & 0 \\ A_{12} & A_{22} & 0 \\ 0 & 0 & A_{66} \end{bmatrix} \begin{Bmatrix} u_{0,r} + \frac{1}{2} w_{0,r}^2 \\ \frac{1}{r} v_{0,\theta} + \frac{1}{r} u_0 + \frac{1}{2r^2} w_{0,\theta}^2 \\ \frac{1}{r} u_{0,\theta} + v_{0,r} - \frac{1}{r} v_0 + \frac{1}{r} w_{0,r} w_{0,\theta} \end{Bmatrix}$$

$$\begin{Bmatrix} M_{rr} \\ M_{\theta\theta} \\ M_{r\theta} \end{Bmatrix} = \begin{bmatrix} D_{11} & D_{12} & 0 \\ D_{12} & D_{22} & 0 \\ 0 & 0 & D_{66} \end{bmatrix} \begin{Bmatrix} \phi_{r,r} \\ \frac{1}{r} \phi_r + \frac{1}{r} \phi_{\theta,\theta} \\ \frac{1}{r} \phi_{r,\theta} + \phi_{\theta,r} - \frac{1}{r} \phi_\theta \end{Bmatrix} \tag{6}$$

$$\begin{Bmatrix} Q_r \\ Q_\theta \end{Bmatrix} = \begin{bmatrix} A_{55} & 0 \\ 0 & A_{44} \end{bmatrix} \begin{Bmatrix} w_{0,r} + \phi_r \\ \frac{1}{r} w_{0,\theta} + \phi_\theta \end{Bmatrix}$$

In the above equations, the constant coefficients A_{ij} and D_{ij} are the stretching and flexural stiffnesses and are obtained in terms of the elasticity modulus, Poisson's ratio, and thickness of the plate as

$$\begin{aligned} A_{11} &= A_{22} = \frac{Eh}{1-v^2}, \quad A_{12} = \frac{vEh}{1-v^2}, \\ A_{44} &= A_{55} = A_{66} = \frac{Eh}{2(1+v)} \\ D_{11} &= D_{22} = \frac{Eh^3}{12(1-v^2)}, \quad D_{12} = \frac{vEh^3}{12(1-v^2)}, \quad D_{66} = \frac{Eh^3}{24(1+v)} \end{aligned} \tag{7}$$

The stress resultants on an element are shown in Figure 2.

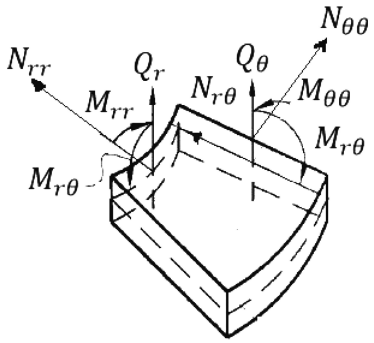

Figure 2 Stress resultants on an element in polar coordinate system.

2.5 Equilibrium Equations

The equilibrium equations of a rotating annular plate under uniform compression may be derived on the basis of the static version of virtual displacements (Reddy, 2003). Considering that the total energy of the plate consists of the strain energy and the potential energy due to the constant rotational speed ω and compressive uniform load $\overline{N}$ on both edges, in an equilibrium position one may write

$$\int_b^a \int_0^{2\pi} \int_{-h/2}^{+h/2} (\sigma_{rr}\delta\varepsilon_{rr} + \sigma_{\theta\theta}\delta\varepsilon_{\theta\theta} + \tau_{r\theta}\delta\gamma_{r\theta} + \tau_{z\theta}\delta\gamma_{z\theta} + \tau_{rz}\delta\gamma_{rz} - \rho r\omega^2\delta u) r dz d\theta dr + \overline{N}\int_0^{2\pi} r\delta u_0 \,|_{r=b}^{r=a}\, d\theta = 0 \tag{8}$$

where $\overline{N}$ is the stress resultant of the applied forces on inner and outer edges of the plate. Integrating the above functional over thickness, recalling Equations (2), (3), and (6), and performing the appropriate mathematical simplifications, a set of equations for the equilibrium state of an annular plate subjected to the simultaneous effects of uniform compression and constant angular speed is obtained as follows

$$\delta u_0 : N_{rr,r} + \frac{1}{r}N_{r\theta,\theta} + \frac{1}{r}(N_{rr} - N_{\theta\theta}) + \rho h r\omega^2 = 0$$
$$\delta v_0 : \frac{1}{r}N_{\theta\theta,\theta} + N_{r\theta,r} + \frac{2}{r}N_{r\theta} = 0$$

$$\begin{aligned}
&\delta w_0 : Q_{r,r} + \frac{1}{r}Q_{\theta,\theta} + \frac{1}{r}Q_r + N_{rr}w_{0,rr} + N_{\theta\theta}\left(\frac{1}{r}w_{0,r} + \frac{1}{r^2}w_{0,\theta\theta}\right) \\
&\qquad +2N_{r\theta}\left(\frac{1}{r}w_{0,r\theta} - \frac{1}{r^2}w_{0,\theta}\right) - \rho h r\omega^2 w_{0,r} = 0 \\
&\delta\phi_r : M_{rr,r} + \frac{1}{r}M_{r\theta,\theta} + \frac{1}{r}(M_{rr} - M_{\theta\theta}) - Q_r = 0 \\
&\delta\phi_\theta : \frac{1}{r}M_{\theta\theta,\theta} + M_{r\theta,r} + \frac{2}{r}M_{r\theta} - Q_\theta = 0
\end{aligned} \tag{9}$$

2.6 Boundary Conditions

The complete set of boundary conditions may be extracted in the process of virtual displacement relieving. In the next, four sets of boundary conditions suitable for the present problem are defined. Accordingly, outer or inner edge of the plate may be simply supported (S), clamped (C), free (F), or sliding support (R). The mathematical expressions for each case are

$$\begin{aligned}
&S : N_{rr} + \overline{N} = N_{r\theta} = w_0 = M_{rr} = \phi_\theta = 0 \\
&C : N_{rr} + \overline{N} = N_{r\theta} = w_0 = \phi_r = \phi_\theta = 0 \\
&F : N_{rr} + \overline{N} = N_{r\theta} = rQ_r + rN_{rr}w_{0,r} + N_{r\theta}w_{0,\theta} = M_{rr} = M_{r\theta} = 0 \\
&R : N_{rr} + \overline{N} = N_{r\theta} = rQ_r + rN_{rr}w_{0,r} + N_{r\theta}w_{0,\theta} = \phi_r = \phi_\theta = 0
\end{aligned} \tag{10}$$

3 Pre-buckling Analysis

Pre-buckling deformations and stresses should be obtained to express the stress state of the plate at the onset and prior to buckling. Consider an isotropic annular plate which is subjected to uniform compression at both inner and outer edges. The plate is also rotating with constant angular speed. The effect of rotation and compression prior to buckling on displacement field is axisymmetric since the applied forces due to rotation and compression and geomety of the plate are axisymmetric. Therefore, the prebuckling deformation of the plate is also axisymmetric.

Only the flat pre-buckling deformations are considered. The pre-buckling deformations of the plate are revealed via the solution of Equation (9), considering only the in-plane displacement components i.e., $w_0^0 = \phi_0^0 = \phi_\theta^0 = 0$. Here a superscript 0 indicates the primary equilibrium path characteristics.

Using three constraints in addition to the axisymmetric condition, only the first and the second of Equation (9) remain, which take the form

$$\begin{aligned} N^0_{rr,r} + \frac{1}{r}(N^0_{rr} - N^0_{\theta\theta}) + \rho h r \omega^2 = 0 \\ N^0_{r\theta,r} + \frac{2}{r} N^0_{r\theta} = 0 \end{aligned} \tag{11}$$

The second equation results in a first order homogeneous ordinary differential equation for $N^0_{r\theta}$ whose solution considering the conditions $N^0_{r\theta}(a) = N^0_{r\theta}(b) = 0$ is $N^0_{r\theta} = 0$. The first equation, however, results in a non-homogeneous second order differential equation for u^0_0 which may be written as

$$\frac{Eh}{1-v^2}\left(\frac{du^{02}_0}{dr^2} + \frac{1}{r}\frac{du^0_0}{dr} - \frac{1}{r^2}u^0_0\right) = -\rho h r w^2 \tag{12}$$

Solution of the above equation considering the boundary conditions $N^0_{rr}(a) = N^0_{rr}(b) = -\overline{N}$ is

$$\begin{aligned} u^0_0 = \frac{\rho w^2}{8E}\Bigg\{(1-v)(3+v)(a^2+b^2)r + (1+v)(3+v)\frac{a^2b^2}{r} \\ -(1-v^2)r^3\Bigg\} - \frac{1-v}{Eh} r\overline{N} \end{aligned} \tag{13}$$

Finally, distribution of force resultants induced due to rotation and compression in the prebuckling regime may be evaluated upon substitution of Equation (13) into Equation (6). The stress resultants in the prebuckling regime are

$$\begin{aligned} N^0_{rr} &= \frac{\rho h \omega^2 (3+v)}{8}\left\{(a^2+b^2) - \frac{a^2b^2}{r^2} - r^2\right\} - \overline{N} \\ N^0_{\theta\theta} &= \frac{\rho h \omega^2 (3+v)}{8}\left\{(a^2+b^2) + \frac{a^2b^2}{r^2} - \frac{1+3v}{3+v}r^2\right\} - \overline{N} \\ N^0_{r\theta} &= 0 \end{aligned} \tag{14}$$

The force resultants induced due to rotation are compatible with those reported in many of the applied mechanics textbooks, see e.g. Hetnarski and Eslami (2009). Further consideration of the prebuckling forces reveal that tangential and radial forces induced due to compression are compressive in the plate domain, while the induced forces due to rotation are both tensile.

4 Stability Equations

The stability equations of an annular plate are derived based on the well- known adjacent-equilibrium criterion. Assume a pre-buckling equilibrium position with displacement components $u_0^0, v_0^0, w_0^0, \phi_r^0$, and ϕ_θ^0. Another equilibrium position may exist, adjacent to the primary one. Displacement components of the secondary equilibrium path differ by arbitrary perturbations $u_0^1, v_0^1, w_0^1, \phi_r^1$, and ϕ_θ^1. Consequently, displacements of the secondary equilibrium path are

$$\begin{aligned} u_0 &= u_0^0 + u_0^1 \\ v_0 &= v_0^0 + v_0^1 \\ w_0 &= w_0^0 + w_0^1 \\ \phi_r &= \phi_r^0 + \phi_r^1 \\ \phi_\theta &= \phi_\theta^0 + \phi_\theta^1 \end{aligned} \tag{15}$$

For the case when perturbation parameters are sufficiently small, displacement field (15) lies on the branching point of the plate. At this stage stability equations may be derived. The stability equations are obtained through usage of Equations (6), (10), (14), and (15). The process is not presented herein for the sake of brevity, nonetheless one may refer to the stability books of Brush and Almroth (1975) and Eslami (2010) for the throughout process of stability equations development.

$$\begin{aligned} &N_{rr,r}^1 + \frac{1}{r}N_{r\theta,\theta}^1 + \frac{1}{r}(N_{rr}^1 - N_{\theta\theta}^1) = 0 \\ &N_{r\theta,r}^1 + \frac{1}{r}N_{\theta\theta,\theta}^1 + \frac{2}{r}N_{r\theta}^1 = 0 \\ &Q_{r,r}^1 + \frac{1}{r}Q_{\theta,\theta}^1 + \frac{1}{r}Q_r^1 + N_{rr}^0 w_{0,rr}^1 + N_{\theta\theta}^1\left(\frac{1}{r}w_{0,r}^1 + \frac{1}{r^2}w_{0,\theta\theta}^1\right) \\ &\quad + 2N_{r\theta}^0\left(\frac{1}{r}w_{0,r\theta}^1 - \frac{1}{r^2}w_{0,\theta}^1\right) - \rho h r\omega^2 w_{0,r}^1 = 0 \\ &M_{rr,r}^1 + \frac{1}{r}M_{r\theta,\theta}^1 + \frac{1}{r}(M_{rr}^1 - M_{\theta\theta}^1) - Q_r^1 = 0 \\ &M_{r\theta,r}^1 + \frac{1}{r}M_{\theta\theta,\theta}^1 + \frac{2}{r}M_{r\theta}^1 - Q_\theta^1 = 0 \end{aligned} \tag{16}$$

The stability equations in terms of the displacement components may be obtained by using Equations (6), (14), and (16) and eliminating the second and

higher order terms of the incremental displacements. The resulting equations are as follow

$$
\begin{aligned}
&A_{11}\left(u^1_{0,rr}+\frac{1}{r}u^1_{0,r}+\frac{1}{r}v^1_{0,r\theta}-\frac{1}{r^2}u^1_0-\frac{1}{r^2}v^1_{0,\theta}\right)\\
&\quad+A_{66}\left(\frac{1}{r^2}u^1_{0,\theta\theta}-\frac{1}{r}v^1_{0,r\theta}-\frac{1}{r^2}v^1_{0,\theta}\right)=0\\
&A_{11}\left(\frac{1}{r}u^1_{0,r\theta}+\frac{1}{r^2}u^1_{0,\theta}+\frac{1}{r^2}v^1_{0,\theta\theta}\right)\\
&\quad+A_{66}\left(-\frac{1}{r^2}u^1_{0,\theta}-\frac{1}{r}u^1_{0,r\theta}+\frac{1}{r}v^1_{0,r}-\frac{1}{r^2}v^1_0+v^1_{0,rr}\right)=0\\
&A_{66}\left(\phi^1_{r,r}+\frac{1}{r}\phi^1_{\theta,\theta}+\frac{1}{r}\phi^1_r+\frac{1}{r^2}w^1_{0,\theta\theta}+w^1_{0,rr}+\frac{1}{r}w^1_{,r}\right)\\
&\quad-\overline{N}\left(w^1_{0,rr}+\frac{1}{r}w^1_{0,r}+\frac{1}{r^2}w^1_{0,\theta\theta}\right)\\
&\quad+\frac{\rho h\omega^2(3+v)}{8}\left\{(a^2+b^2)-\frac{a^2b^2}{r^2}-r^2\right\}w^1_{0,rr}-\rho hr\omega^2w^1_{0,r}\\
&\quad+\frac{\rho h\omega^2(3+v)}{8}\left\{(a^2+b^2)-\frac{a^2b^2}{r^2}-\frac{1+3v}{3+v}r^2\right\}\\
&\quad\left(\frac{1}{r}w^1_{0,r}+\frac{1}{r^2}w^1_{0,\theta\theta}\right)=0\\
&D_{11}\left(\phi^1_{r,rr}+\frac{1}{r}\phi^1_{r,r}+\frac{1}{r}\phi^1_{\theta,r\theta}-\frac{1}{r^2}\phi^1_r-\frac{1}{r^2}\phi^1_{\theta,\theta}\right)\\
&\quad+D_{66}\left(\frac{1}{r^2}\phi^1_{r,\theta\theta}-\frac{1}{r}\phi^1_{\theta,r\theta}-\frac{1}{r^2}\phi^1_{\theta,\theta}\right)-A_{66}(\phi^1_r+w^1_{0,r})=0\\
&D_{11}\left(\frac{1}{r}\phi^1_{r,r\theta}+\frac{1}{r^2}\phi^1_{r,\theta}+\frac{1}{r^2}\phi^1_{\theta,\theta\theta}\right)\\
&\quad+D_{66}\left(\frac{1}{r^2}\phi^1_{r,\theta}-\frac{1}{r}\phi^1_{r,r\theta}+\frac{1}{r}\phi^1_{\theta,r}-\frac{1}{r^2}\phi^1_\theta+\phi^1_{\theta,rr}\right)\\
&\quad-A_{66}\left(\phi^1_\theta+\frac{1}{r}w^1_{0,\theta}\right)=0
\end{aligned}
\tag{17}
$$

The above system of equations are five partial differential equations where the first two of them are independent of the other three. Therefore, to obtain the buckling state of the plate, only the last three ones may be considered. In the next, a solution method for the last three stability equations is provided.

5 Solution Procedure

Due to the periodical conditions of the displacement field and considering the fact that the buckling state of the annular plate may be asymmetric (Bagheri et al., 2017b; Ghiasian et al., 2014; Kiani and Eslami, 2013a, 2013b), the solution of the displacement field components is considered in the next form

$$\begin{aligned} w_0^1(r,\theta) &= W_n(r)\cos(n\theta) \\ \varphi_0^1(r,\theta) &= \Phi_n(r)\cos(n\theta) \\ \varphi_0^1(r,\theta) &= \Psi_n(r)\sin(n\theta) \end{aligned} \tag{18}$$

where n is the number of nodal diameters. Substitution of Equation (18) into the last three stability equations from Equation (17) yield

$$\begin{aligned} &A_{66}\left(\Phi_{n,r}+\frac{n}{r}\Psi_n+\frac{1}{r}\Phi_n-\frac{n^2}{r^2}W_n+W_{n,rr}+\frac{1}{r}W_{n,r}\right) \\ &\quad-\overline{N}\left(W_{n,rr}+\frac{1}{r}W_{n,r}-\frac{n^2}{r^2}W_n\right) \\ &\quad+\frac{\rho h\omega^2(3+v)}{8}\left\{(a^2+b^2)-\frac{a^2b^2}{r^2}-r^2\right\}W_{n,rr}-\rho hr\omega^2W_{n,r} \\ &\quad+\frac{\rho h\omega^2(3+v)}{8}\left\{(a^2+b^2)+\frac{a^2b^2}{r^2}-\frac{1+3v}{3+v}r^2\right\}\left(\frac{1}{r}W_{n,r}-\frac{n^2}{r^2}W_n\right)=0 \\ &D_{11}\left(\Phi_{n,rr}+\frac{1}{r}\Phi_{n,r}+\frac{n}{r}\Psi_{n,r}-\frac{1}{r^2}\Phi_n-\frac{n}{r^2}\Psi_n\right) \\ &\quad+D_{66}\left(-\frac{n^2}{r^2}\Phi_n-\frac{n}{r}\Psi_{n,r}-\frac{n}{r^2}\Psi_n\right)-A_{66}(\Phi_n+W_{n,r})=0 \end{aligned}$$

$$
\begin{aligned}
&D_{11}\left(-\frac{n}{r}\Phi_{n,r}-\frac{n}{r^2}\Phi_n-\frac{n^2}{r^2}\Psi_n\right)\\
&\quad+D_{66}\left(-\frac{n}{r^2}\Phi_n+\frac{n}{r}\Phi_{n,r}+\frac{1}{r}\Psi_{n,r}-\frac{1}{r^2}\Psi_n+\Psi_{n,rr}\right)\\
&\quad-A_{66}\left(\Psi_n+\frac{1}{r}W_n\right)=0
\end{aligned}
\tag{19}
$$

The above three equations are coupled and homogeneous. In the next, for the sake of generality, equations are transformed into a dimensionless presentation. The following non-dimensional parameters are used in the rest of this work

$$
\begin{aligned}
&\mu=\frac{2}{1-v},\quad s=\frac{r}{a},\quad \delta=\frac{h}{a},\quad \overline{W}=\frac{W}{a},\quad \beta=\frac{b}{a},\\
&\lambda=\frac{12(1-v^2)\overline{N}a^2}{Eh^3},\quad \chi^2=\frac{12(1-v^2)\rho h\omega^2a^4}{Eh^3},
\end{aligned}
\tag{20}
$$

With the aid of the newly defined parameters (20), the stability equations in a dimensionless presentation take the form

$$
\begin{aligned}
&\Phi_{n,s}+\frac{n}{s}\Psi_n+\frac{1}{s}\Phi_n-\frac{n^2}{s^2}\overline{W}_n+\overline{W}_{n,ss}+\frac{1}{s}\overline{W}_{n,s}\\
&\quad-\frac{1}{12}\mu\delta^2\lambda\left(\overline{W}_{n,ss}+\frac{1}{s}\overline{W}_{n,s}-\frac{n^2}{s^2}\overline{W}_n\right)\\
&\quad+\frac{\mu\delta^2\chi^2(3+v)}{96}\left\{(1+\beta^2)-\frac{\beta^2}{s^2}-s^2\right\}\overline{W}_{n,ss}-\frac{\mu\delta^2\chi^2}{12}s\overline{W}_{n,s}\\
&\quad+\frac{\mu\delta^2\chi^2(3+v)}{96}\left\{(1+\beta^2)+\frac{\beta^2}{s^2}-\frac{1+3v}{3+v}s^2\right\}\left(\frac{1}{s}\overline{W}_{n,s}-\frac{n^2}{s^2}\overline{W}_n\right)=0\\
&\frac{\delta^2}{12}\left(\mu\Phi_{n,ss}+\frac{\mu}{s}\Phi_{n,s}+\frac{n}{s}(\mu-1)\Psi_{n,s}-\left(\frac{12}{\delta^2}+\frac{\mu+n^2}{s^2}\right)\Phi_n\right.\\
&\quad\left.-\frac{n}{s^2}(\mu+1)\Psi_n\right)-\overline{W}_{n,s}=0\\
&\frac{\delta^2}{12}\left(\Psi_{n,ss}+\frac{1}{s}\Psi_{n,s}-\frac{n}{s}(\mu-1)\Phi_{n,s}-\left(\frac{12}{\delta^2}+\frac{\mu n^2+1}{s^2}\right)\Psi_n\right.\\
&\quad\left.-\frac{n}{s^2}(\mu+1)\Phi_n\right)+\frac{n}{s}\overline{W}_n=0
\end{aligned}
\tag{21}
$$

The above system of equations are coupled with non-constant coefficients. Obtaining an analytical solution for such equations is complicated and therefore a numerical solution should be employed. Here, the generalised differential quadratures (GDQ) method is used to discretize the system of Equations (21) through the radius of the plate. Distribution of nodal points is obtained based on the well-known Chebyshev-Gauss-Lobatto method as

$$s_i = \beta + \frac{1-\beta}{2}\left\{1 - \cos\left(\frac{i-1}{N-1}\pi\right)\right\}, \quad i = 1, 2, \ldots, N \tag{22}$$

Applying the GDQ method to the stability Equations (21) and the boundary conditions (11), results in a system of algebraic eigenvalue problem. Process is not presented herein nonetheless one may refer to (Shu, 2000) for more details. When the radial domain of the plate, i.e., $\beta < s < 1$ is divided into N nodes, the discreted form of the stability Equations (21) may be expressed as

$$\begin{aligned}
&\left(\sum_{j=1}^{N} C_{ij}^{(1)} + \frac{1}{s_i}\sum_{j=1}^{N} C_{ij}^{(0)}\right)\Phi_{nj} + \frac{n}{s_i}\sum_{j=1}^{N} C_{ij}^{(0)}\Psi_{nj} \\
&+ \left(\sum_{j=1}^{N} C_{ij}^{(2)} + \frac{1}{s_i}\sum_{j=1}^{N} C_{ij}^{(1)} - \frac{n^2}{s_i^2}\sum_{j=1}^{N} C_{ij}^{(0)}\right)\overline{W}_{nj} \\
&- \frac{1}{12}\mu\delta^2\lambda\left(\sum_{j=1}^{N} C_{ij}^{(2)} + \frac{1}{s_i}\sum_{j=1}^{N} C_{ij}^{(1)} - \frac{n^2}{s_i^2}\sum_{j=1}^{N} C_{ij}^{(0)}\right)\overline{W}_{nj} \\
&+ \frac{\mu\delta^2\chi^2(3+v)}{96}\left((1+\beta^2) - \frac{\beta^2}{s_i^2} - s_i^2\right)\sum_{j=1}^{N} C_{ij}^{(2)}\overline{W}_{nj} \\
&- \frac{\mu\delta^2\chi^2}{12}s_i\sum_{j=1}^{N} C_{ij}^{(1)}\overline{W}_{nj} + \frac{\mu\delta^2\chi^2(3+v)}{96} \\
&\left((1+\beta^2) + \frac{\beta^2}{s_i^2} - \frac{1+3v}{3+v}s_i^2\right) \\
&\left(\frac{1}{s_i}\sum_{j=1}^{N} C_{ij}^{(1)}\overline{W}_{nj} - \frac{n^2}{s_i^2}\sum_{j=1}^{N} C_{ij}^{(0)}\overline{W}_{nj}\right) = 0
\end{aligned}$$

$$\frac{\delta^2}{12}\left(\mu\sum_{j=1}^{N}C_{ij}^{(2)}+\frac{\mu}{s_i}\sum_{j=1}^{N}C_{ij}^{(1)}-\left(\frac{12}{\delta^2}+\frac{\mu+n^2}{s_i^2}\right)\sum_{j=1}^{N}C_{ij}^{(0)}\right)\Phi_{nj}$$
$$+\frac{\delta^2}{12}\left(\frac{n}{s_i}(\mu-1)\sum_{j=1}^{N}C_{ij}^{(1)}-\frac{n}{s_i^2}(\mu+1)\sum_{j=1}^{N}C_{ij}^{(0)}\right)\Psi_{nj}$$
$$-\sum_{j=1}^{N}C_{ij}^{(1)}\overline{W}_{nj}=0$$
$$\frac{\delta^2}{12}\left(\sum_{j=1}^{N}C_{ij}^{(2)}+\frac{1}{s_i}\sum_{j=1}^{N}C_{ij}^{(1)}-\left(\frac{12}{\delta^2}+\frac{\mu+n^2}{s_i^2}\right)\sum_{j=1}^{N}C_{ij}^{(0)}\right)\Psi_{nj}$$
$$-\frac{\delta^2}{12}\left(\frac{n}{s_i}(\mu-1)\sum_{j=1}^{N}C_{ij}^{(1)}+\frac{n}{s_i^2}(\mu+1)\sum_{j=1}^{N}C_{ij}^{(0)}\right)\Phi_{nj}$$
$$+\frac{n}{s_i}\sum_{j=1}^{N}C_{ij}^{(0)}\overline{W}_{nj}=0 \tag{23}$$

where in the above equations $i = 1, 2, \ldots, N$ and $C^{(r)}$ stands for the r-th. derivative coefficients in the GDQ method. After applying the GDQ method to the boundary conditions, Equation (23) in a compact form may be written as

$$(\mathbf{K}_E - \lambda\mathbf{K}_N - \chi^2\mathbf{K}_\omega)\mathbf{X} = 0 \tag{24}$$

In Equation (24) $\mathbf{K}_E$ is the elastic stiffness matrix, $\mathbf{K}_N$ is the geometrical stiffness matrix due to uniform compression, and $\mathbf{K}_\omega$ is the geometrical stiffness matrix due to rotation. The above system should be solved as an eigenvalue problem to obtain the critical states of the plate and the associated buckled shapes. In this study a Matlab code is developed to obtain the eigenvalues and eigenvectors. In this code, the eigenvalues and eigenvectors of the system of equations are obtained based on the Lanczos algorithm. The process to obtain those parameters is as follows: For each circumferential mode number n starting from zero, the eigenvalue problem is solved and the minimum eigenvalue which is n^T is obtained. Searching among all of these minimums which are extracted for different number of nodal diameters and choosing the minimum one, one may reach to

the critical buckling parameter of the plate n_{cr}^{T} and the associated mode number n.

6 Numerical Investigation

The procedure outlined in the previous sections is used herein to obtain the critical states of a rotating annular plate subjected to uniform compression on both inner and outer edges. Different combinations of boundary conditions are considered. Following convention is used for the boundary conditions. For instance a plate which is clamped at the inner edge and simply supported at the outer edge is denoted by C-S. In the procedure of solution and the numerical results, the number of nodal points in GDQ method is chosen as $N = 32$, after examination of convergence up to 3 digits. In whole of the numerical studies the Poisson ratio is set equal to $\nu = 0.3$.

In this section, first, comparison studies are provided to assure the validity and accuracy of the present formulation. Afterwards, parametric studies are provided to explore the simultaneous effects of rotation and uniform compression on the buckling states of the plate.

6.1 Comparison Studies

A comparison study is provided in this section. A study is conducted for the case of a stationary annular plate subjected to pure compression. Yamaki (1985) and Wang et al. (2004) obtained the critical buckling loads of thin annular plates using the classical plate theory. Results of this study are compared with those of Wang et al. (2004). For the sake of comparison, a thin plate is considered and therefore $\delta = 0.001$ is considered for generation of the present numerical results. Comparison is provided in Table 1 for various values of β ratio. It is observed that for all types of boundary conditions and inner to outer radius ratio, the results of our study are in excellent agreement with those of Wang et al. (2004). Further investigation of the numerical results indicates that the fundamental buckling shape of an annular plate subjected to pure compression may be asymmetric. For plates with both edges clamped, the fundamental buckling pattern is always asymmetric which is designated with number of nodal diameters greater than zero. Furthermore, unlike the other combinations of boundary conditions, in the S-F and F-S plates variation of buckling load with respect to hole size is not monotonic. For other combinations of boundary conditions, with increasing the β ratio, critical buckling load of the plate increases. However, for these two types trend is not monotonic.

Table 1 Comparison of non-dimensional critical buckling load parameter of stationary annular plates $\sqrt{\lambda_{cr}}$ between the results of this study and those of Wang et al. (2004). Numbers in parenthesis indicate the number of nodal diameters

Boundary Conditions	Source	$\beta = 0.1$	$\beta = 0.3$	$\beta = 0.5$	$\beta = 0.7$	$\beta = 0.9$
C-C	Present	6.71 (1)	8.63 (2)	12.15 (4)	20.28 (7)	60.85 (23)
	Wang et al. (2004)	6.68 (2)	8.63 (2)	12.15 (4)	20.27 (7)	60.89 (24)
S-S	Present	4.20 (0)	4.75 (0)	6.40 (0)	10.52 (0)	31.44 (1)
	Wang et al. (2004)	4.20 (1)	4.75 (0)	6.40 (0)	10.52 (0)	31.43 (0)
C-S	Present	4.69 (1)	6.15 (0)	8.72 (0)	14.72 (0)	44.67 (0)
	Wang et al. (2004)	4.71 (1)	6.16 (0)	8.73 (0)	14.73 (0)	44.69 (0)
S-C	Present	5.99 (1)	7.06 (0)	9.42 (0)	15.30 (0)	44.19 (0)
	Wang et al. (2004)	6.02 (1)	7.06 (0)	9.42 (0)	15.31 (0)	45.20 (0)
F-C	Present	3.62 (0)	3.19 (0)	3.65 (0)	5.52 (0)	15.87 (0)
	Wang et al. (2004)	3.62 (0)	3.19 (0)	3.65 (0)	5.52 (0)	15.87 (0)
R-C	Present	3.94 (0)	4.71 (0)	6.39 (0)	10.52 (0)	31.43 (0)
	Wang et al. (2004)	3.94 (0)	4.71 (0)	6.39 (0)	10.49 (0)	30.45 (12)
F-S	Present	1.98 (0)	1.61 (0)	1.32 (0)	1.14 (0)	1.01 (0)
	Wang et al. (2004)	1.98 (0)	1.61 (0)	1.32 (0)	1.14 (0)	1.01 (0)
R-S	Present	2.09 (0)	2.40 (0)	3.18 (0)	5.19 (0)	15.60 (0)
	Wang et al. (2004)	2.09 (0)	2.40 (0)	3.18 (0)	5.19 (0)	15.61 (0)
C-F	Present	1.49 (0)	2.40 (0)	3.14 (0)	5.19 (0)	15.60 (0)
	Wang et al. (2004)	1.49 (0)	2.40 (0)	3.14 (0)	5.19 (0)	15.61 (0)
S-F	Present	1.13 (0)	1.34 (0)	1.32 (0)	1.14 (0)	1.01 (0)
	Wang et al. (2004)	1.13 (0)	1.34 (0)	1.32 (0)	1.14 (0)	1.01 (0)

6.2 Parametric Studies

After validating the proposed formulation for the case of stationary annular plates, parametric studies are presented to explore the buckling states of a rotating annular plate subjected to uniform compression. Results of this section are provided in Figures 3–10.

Figures 3–8 provide the critical buckling load of a rotating annular plate with respect to rotating speed. These figures are associated to C-C, C-F, C-S, F-C, S-C, and S-S boundary conditions, respectively. In each case, various hole sizes and different thickness ratios are considered. It is observed that, in all cases, rotation enhances the buckling load of the plate. Such trend is expected since the forces induced due to rotation are tensile in the plate. Therefore, with increasing the rotating speed, compressive buckling load of the plate increases significantly. Increment ratio of the buckling load for different β ratios is not the same. For instance, as the present results reveal in an S-C plate buckling load of a stationary plate with hole size $\beta = 0.5$ is higher than a plate with

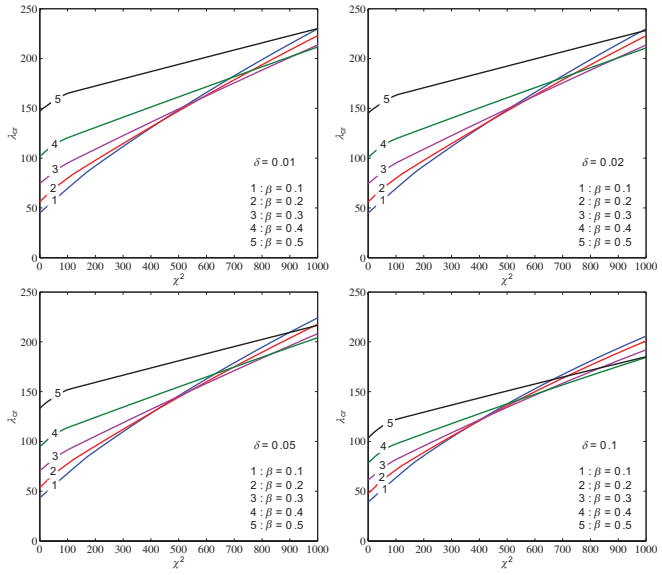

Figure 3 Compressive buckling load parameter as a function of rotation parameter for the C-C boundary conditions, different thickness to outer radius ratios, and various inner to outer radius ratios.

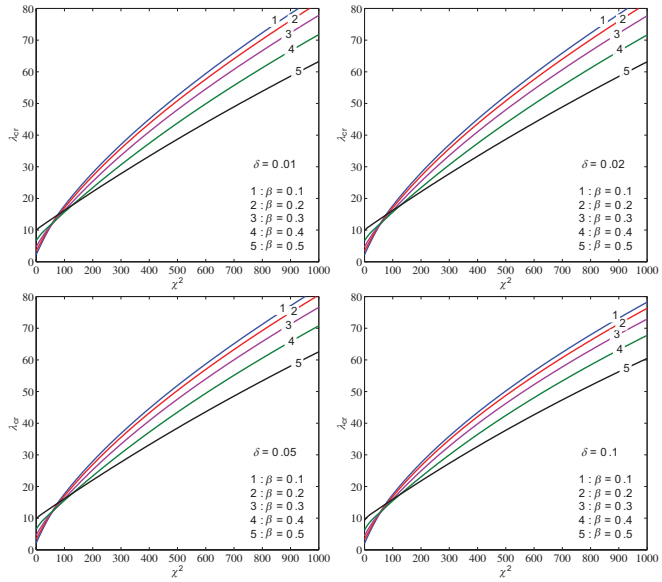

Figure 4 Compressive buckling load parameter as a function of rotation parameter for the C-F boundary conditions, different thickness to outer radius ratios, and various inner to outer radius ratios.

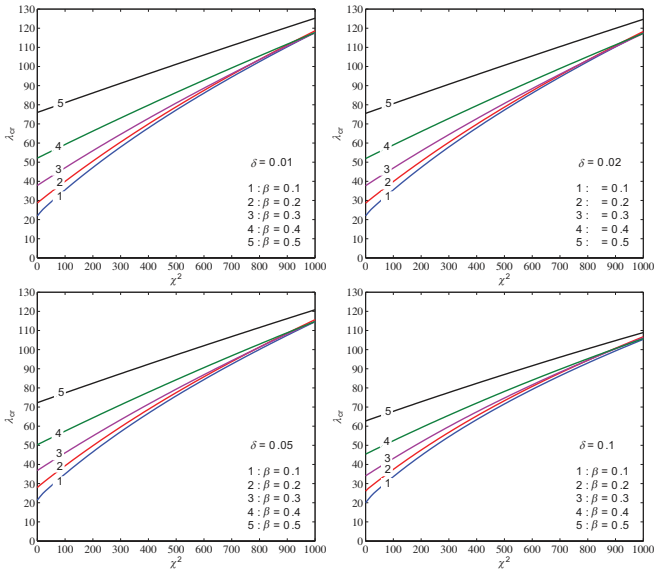

Figure 5 Compressive buckling load parameter as a function of rotation parameter for the C-S boundary conditions, different thickness to outer radius ratios, and various inner to outer radius ratios.

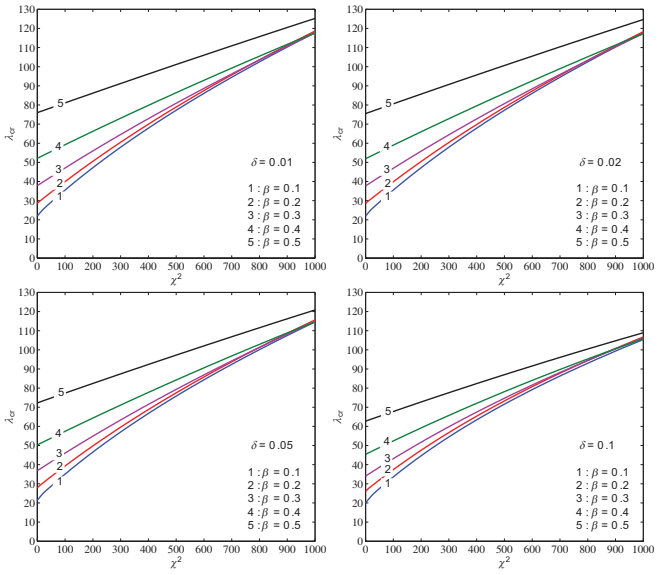

Figure 6 Compressive buckling load parameter as a function of rotation parameter for the F-C boundary conditions, different thickness to outer radius ratios, and various inner to outer radius ratios.

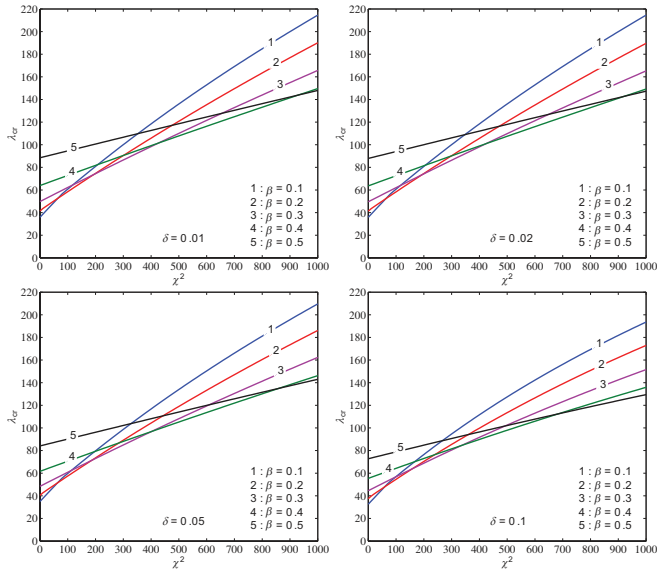

Figure 7 Compressive buckling load parameter as a function of rotation parameter for the S-C boundary conditions, different thickness to outer radius ratios, and various inner to outer radius ratios.

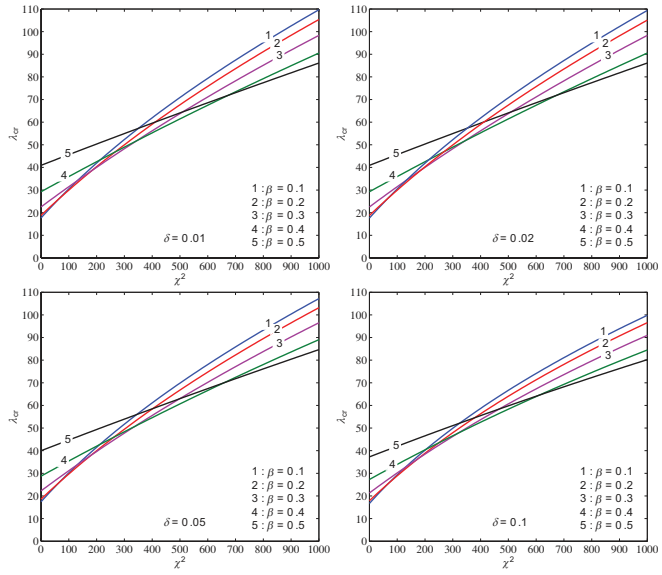

Figure 8 Compressive buckling load parameter as a function of rotation parameter for the S-S boundary conditions, different thickness to outer radius ratios, and various inner to outer radius ratios.

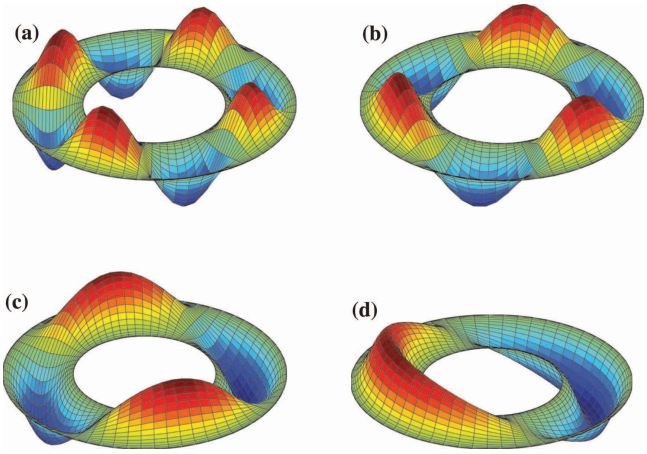

Figure 9 Buckling configuration of the C-C annular plates with $\beta = 0.5$ and $\delta = 0.05$. (a) $\chi^2 = 0, \lambda_{cr} = 133.126, n = 4$, (b) $\chi^2 = 50, \lambda_{cr} = 144.145, n = 3$, (c) $\chi^2 = 75, \lambda_{cr} = 148.606, n = 2$, (d) $\chi^2 = 100, \lambda_{cr} = 151.824, n = 1$.

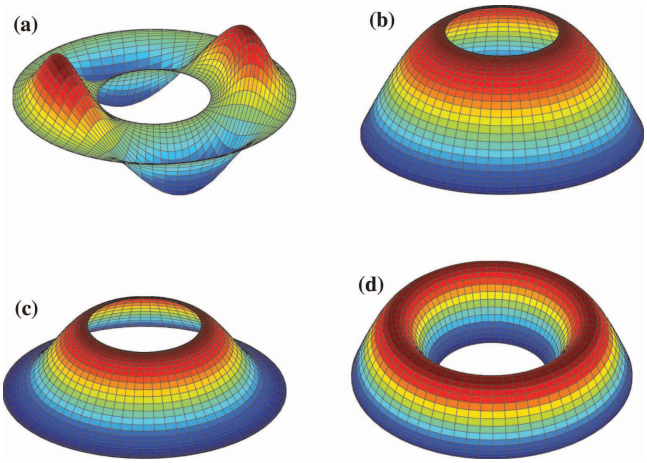

Figure 10 Buckling configuration of the annular plates with $\beta = 0.4$, $\delta = 0.05$ and $\chi^2 = 50$. (a) C-C, $\lambda_{cr} = 105.908, n = 2$, (b) C-F, $\lambda_{cr} = 11.546, n = 0$, (c) C-R $\lambda_{cr} = 34.852, n = 0$, (d) S-S, $\lambda_{cr} = 32.117, n = 0$.

$\beta = 0.1$. On the other hand, with the introduction of rotation, trend changes. For rotating speed $\chi^2 > 300$, buckling load of a rotating plate with hole size $\beta = 0.1$ is higher than a plate with $\beta = 0.5$.

The GDQ method, similar to the finite elements or finite difference methods, discretizes the governing equations and yields the lateral deflections

at each radial line. Since the total shape of the plate is $W(r)\sin(n\theta)$, it is easy to plot the shapes of the plate at the onset of buckling. To this end, once the eigenvalue problem is solved and the minimum buckled shape of the plate is obtained, the number of nodal diameters for this load n and the eigenvector of the plate are revealed. The eigenvector of the plate consist of $3N$ components where N of them are the nodal magnitudes of defection. Thus, the peicewise function $W(r)$ at the onset of buckling is known. Therefore, one may plot $W(r)\sin(n\theta)$ in the polar coordinates. Following this explanation, a schematic of fundamental buckling pattern of annular plates is provided in Figure 9. Results are given for various values of rotating speed for a plate with both edges clamped, $\beta = 0.5$ and $\delta = 0.05$. It is observed that critical buckling load of the plate increases with increasing the rotating speed. Furthermore, rotation may change the buckling pattern of an annular plate. As seen, the number of nodal diameters changes from 4 to 3 when rotating speed increases from $\chi^2 = 0$ to $\chi^2 = 50$. Further examination reveals that the buckling mode number is $n = 1$ up to $\chi^2 = 110$. For $\chi^2 > 110$ the mode number at the onset of buckling is equal to $n = 0$.

Figure 10 presents the fundamental buckling pattern of rotating annular plates with different rotating speed where $\beta = 0.4, \delta = 0.05$, and $\chi^2 = 50$. It is observed that for the C-F, C-R, and S-S boundary conditions, the buckling pattern is axisymmetric. For a C-C plate, the buckling pattern is associated with the number of nodal diameters $n = 2$. It is verified that essential boundary conditions are satisfied at the supports.

7 Conclusion

Present study aims to obtain the accurate buckling loads and buckled shape of a rotating annular plate subjected to uniform compression on both inner and outer edges. Plate is made from an isotropic and homogeneous material. First order shear deformation plate theory is used to estimate the plate kinematics. An axisymmetric flatness pre-buckling analysis is performed. Stability equations are obtained according the adjacent equilibrium criterion. The resulting equations are discreted via the generalised differential quadrature method. The followings are the general conclusions extracted from the numerical results.

- The fundamental buckling pattern of a rotating/stationary annular plate subjected to axisymmetric uniform compression may be asymmetric.
- The fundamental buckling pattern of stationary C-C plates is always asymmetric.

- Except for the S-F and F-S plates, the fundamental buckling load of annular plates with other combinations of boundary conditions increases with the increase of the hole size.
- Increasing the rotation speed increases the buckling loads of the annular plate subjected to uniform compression. This is due to the tensile nature of the force resultants induced by the rotation.
- Rotation alters the distribution of the stresses within the plate in pre-buckling regime and may change the buckling pattern of the plate in both radial and circumferential directions.

Disclosure Statement

No potential conflict of interest was reported by the authors.

ORCID

Y. Kiani – http://orcid.org/0000-0003-1428-0034

References

Adams, G. G. (1987). Critical speeds for a flexible spinning disk. *International Journal of Mechanical Sciences*, 29(8), 525–531.

Bagheri, H., Kiani, Y., and Eslami, M. R. (2017a). Asymmetric thermo-inertial buckling of annular plates. *Acta Mechanica*, 228(4), 493–509.

Bagheri, H., Kiani, Y., and Eslami, M. R. (2017b). Asymmetric thermal buckling of annular plates on a partial elastic foundation. *Journal of Thermal Stresses*, 40(8), 1015–1029.

Bauer, H. F. and Eidel, W. (2007). Transverse vibration and stability of spinning circular plates of constant thickness and different boundary conditions. *Journal of Sound and Vibration*, 300(3–5), 877–895.

Brush, D. O. and Almroth, B. O. (1975). *Buckling of bars, plates, and shells.* New York: McGraw-Hill.

Eid, H. and Adams, G. G. (2006). Critical speeds and the response of a spinning disk to a stationary load using Mindlin plate theory. *Journal of Sound and Vibration*, 290(1–2), 209–222.

Eslami, M. R. (2010). *Thermo-mechanical buckling of composite plates and shells.* Tehran: Amirkabir University Press.

Ghiasian, S. E., Kiani, Y., Sadighi, M., and Eslami, M. R. (2014). Thermal buckling of shear deformable temperature dependent circular annular FGM plates. *International Journal of Mechanical Sciences*, 81, 137–148.

Hetnarski, R. B. and Eslami, M. R. (2009). *Thermal stresses, advanced theory and applications.* Amsterdam: Springer.

Irie, T., Yamada, G., and Tsujino, M. (1982). Vibration and stability of a variable thickness annular plates subjected to a torque. *Journal of Sound and Vibration*, 85(2), 277–285.

Iwan, W. D. and Moeller, T. L. (1976). The stability of a spinning elastic disk with a transverse load system. *Journal of Applied Mechanics*, 43(3), 485–490.

Kiani, Y. and Eslami, M. R. (2013a). An exact solution for thermal buckling of annular plate on an elastic medium. *Composites Part B: Engineering*, 45(1), 101–110.

Kiani, Y. and Eslami, M. R. (2013b). Instability of heated circular FGM plates on a partial Winkler-type foundation. *Acta Mechanica*, 224(5), 1045–1060.

Kiani, Y. and Eslami, M. R. (2014). Nonlinear thermo-inertial stability of thin circular FGM plates. *Journal of the Franklin Institute*, 351(2), 1057–1073.

Majumdar, S. (1971). Buckling of a thin annular plate under uniform compression. *AIAA Journal*, 9(9), 1701–1707.

Maretic, R. (1998). Vibration and stability of rotating plates with elastic edge supports. *Journal of Sound and Vibration*, 210(2), 291–294.

Maretic, R. B. and Glavardanov, V. B. (2004). Stability of a rotating heated circular plate with elastic edge support. *Journal of Applied Mechanics*, 71(6), 896–899.

Maretic, R. B., Glavardanov, V. B., and Radomirovic, D. (2007). Asymmetric vibrations and stability of a rotating annular plate loaded by a torque. *Meccanica*, 42(6), 537–546.

Mostaghel, N. and Tadjbakhsh, I. (1973). Buckling of rotating rods and plates. *International Journal of Mechanical Sciences*, 15(6), 429–443.

Reddy, J. N. (2003). *Mechanics of laminated composite plates and shells, theory and application.* New York: CRC Press.

Shu, C. (2000). *Differential quadrature and its application in engineering.* London: Springer.

Tutunku, N. (2000). Effect of anisotropy on inertio-elastic instability of rotating disks. *International Journal of Solids and Structures*, 37(51), 7609–7616.

Tutunku, N. and Durdu, A. (1998). Determination of buckling speed for rotating ortho- tropic disk restrained at outer edge. *AIAA Journal*, 36(1), 89–93.

Wang, C. M., Wang, C. Y., and Reddy, J. N. (2004). *Exact solutions for buckling of structural members.* Boca Raton: CRC Press.

Yamaki, N. (1985). Buckling of a thin annular plate under uniform compression. *Journal of Applied Mechanics*, 25, 267–273.